Numerical Solution for a Transient Temperature Distribution on a Finite Domain Due to a Dithering or Rotating Laser Beam

Tsuwei Tan, Department of Applied Mathematics, Naval Postgraduate School, Monterey, CA, USA

Hong Zhou, Department of Applied Mathematics, Naval Postgraduate School, Monterey, CA, USA

ABSTRACT

The temperature distribution due to a rotating or dithering Gaussian laser beam on a finite body is obtained numerically. The authors apply various techniques to solve the nonhomogeneous heat equation in different spatial dimensions. The authors' approach includes the Crank-Nicolson method, the Fast Fourier Transform (FFT) method and the commercial software COMSOL. It is found that the maximum temperature rise decreases as the frequency of the rotating or dithering laser beam increases and the temperature rise induced by a rotating beam is smaller than the one induced by a dithering beam. The authors' numerical results also provide the asymptotic behavior of the maximum temperature rise as a function of the frequency of a rotating or dithering laser beam.

Keywords: *Crank-Nicolson, Fast, Fourier Transform (FFT), Nonhomogeneous Heat Equation, Rotating or Dithering Gaussian Laser Beam*

INTRODUCTION

The impact of laser beams on metals or other materials is of great interest in industry and military. This is mainly due to the fast processing time and precise operation. A deeper understanding of the physics requires a modeling of the heating process. There are many previous works on the theoretical and numerical modeling of temperature profiles induced by laser radation in solids (Araya & Gutierrez, 2006; Bertolotti & Sibilia., 1981; Burgener & Reedy, 1982; Calder & Sue, 1982; Cline & Anthony, 1977; Lax, 1977 and 1978; Moody & Hendel, 1982; Sanders, 1984). However, most of these studies are limited to a scanning Gaussian beam. Until

DOI: 10.4018/ijoris.2013100102

Figure 1. (1) A dithering laser beam on a 1-D rod. (2) 1-D temperature distribution along the rod from various numerical methods. (3) 1D maximum temperature rise of steel AISI 4340 versus frequency of the dithering laser beam. (4) The curve in (3) is well approximated by the function $T_{\max} = 137.0864/\text{frequency} + 51.6960$.

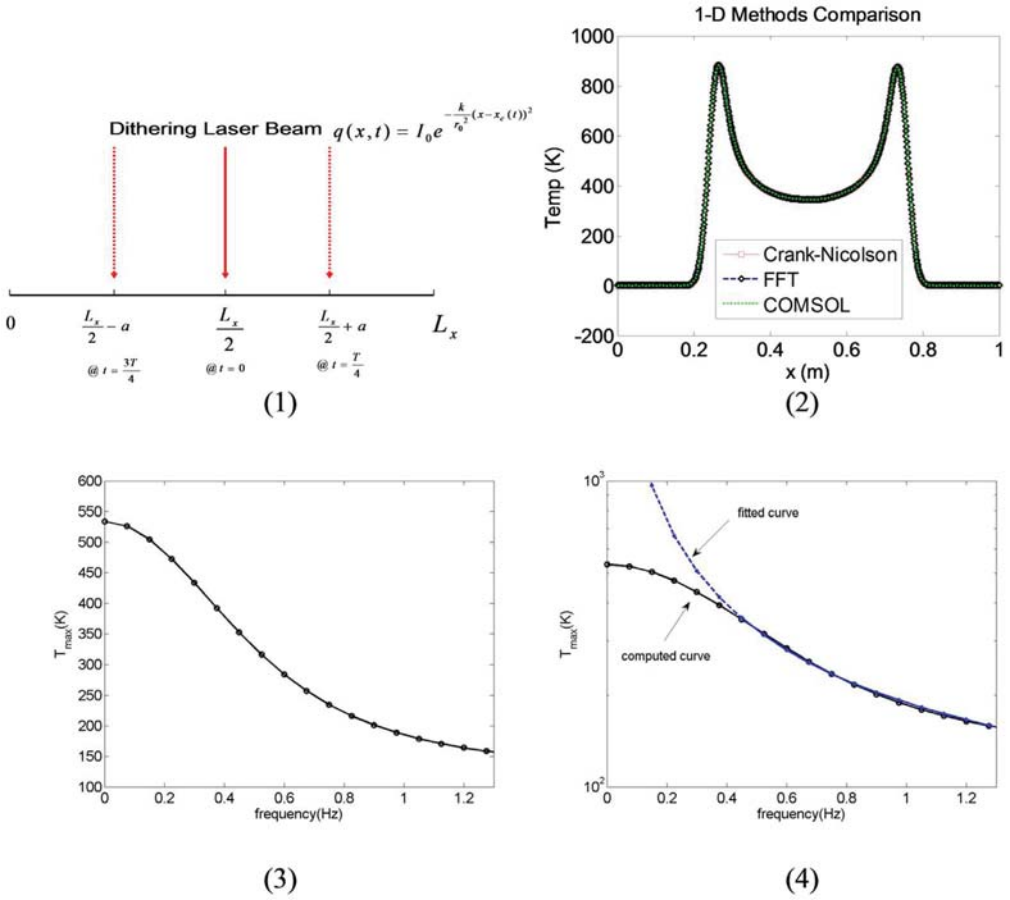

recently laser forming of plates using a rotating or dithering laser beam has been studied (Sistaninia et al., 2009). A more detailed study of the temperature rise induced by a rotating or dithering laser beam on a semi-infinite domain is newly provided by Zhou (2011). In this paper we want to extend the study in Zhou (2011) to a more realistic finite geometry and figure out the quantitative relationship between the maximum temperature rise and the frequency of the rotating or dithering laser beam.

It should be pointed out that the models used here are heat equations, which are deterministic. In order to be able to include random effects (e.g. laser beam jitter) it is desirable to use stochastic differential equations instead of heat equations. This will be the direction of future work.

We organize our paper into five sections. In the first four sections we present the numerical modeling of the temperature distributions induced by a dithering or rotating laser beam in one-dimensional, two-dimensional and three-dimensional finite solids, respectively. Conclusions and future work are given in the last section.

1-D MATHEMATICAL MODELING

Consider a laser beam hitting a 1-D rod with finite length L. The beam moves along the rod which is insulated at the two endpoints. Mathematically, the temperature distribution of the rod can be modeled by the nonhomogeneous heat equation:

$$\frac{\partial u}{\partial t} = \alpha_T \frac{\partial^2 u}{\partial x^2} + \frac{\alpha_T}{K_T} q(x,t), \tag{1}$$

where $u(x,t)$ denotes the temperature rise of the rod at position x $(0 \le x \le L)$ and time t, α_T is the thermal diffusivity of the rod, K_T is the thermal conductivity, and $q(x,t)$ is the energy distribution of the moving laser beam. In the case of a dithering laser beam shown in Figure 1 (1), $q(x,t)$ can be expressed as

$$q(x,t) = \frac{I_0}{r_0} \exp\left[-\frac{k}{r_0^2}\left(x - x_c(t)\right)^2\right],$$
$$x_c(t) = x_0 + a \sin\frac{2\pi t}{T}, \tag{2}$$

where $x_c(t)$ is the position of the dithering Gaussian beam, x_0 is the initial position of the laser beam, I_0 is the intensity of the laser beam, r_0 is the effective radius of the laser beam, and k is a constant used for the Gaussian model. The initial condition for $u(x,t)$ is zero which assumes that the rod has the same temperature as the ambient initially. The boundary conditions impose that the rod is insulated at the two ends:

$$\left.\frac{\partial u}{\partial x}\right|_{x=0} = \left.\frac{\partial u}{\partial x}\right|_{x=L} = 0. \tag{3}$$

The boundary conditions reflect the assumption that no energy escapes into the ambient at the air/rod interface. This is a good approximation for most materials under consideration because heat flow by conduction through the material is much larger than heat loss by radiation or convection at the air/material interface.

An analytical solution based on the eigenfunction expansion can be derived for this initial-boundary value problem. Assume

$$u(x,t) = \sum_n u_n(t) X_n(x), \quad q(x,t) = \sum_n q_n(t) X_n(x), \tag{4}$$

where $X_n(x) = \cos\left(\frac{n\pi x}{L}\right)$ $(n = 1,2,\cdots)$ are the eigenfunctions. After substituting (4) into (1), one has

$$u_n'(t) + \alpha_T \left(\frac{n\pi}{L}\right)^2 u_n(t) = \frac{\alpha_T}{K_T} q_n(t), \tag{5}$$

with the initial condition $u_n(0) = 0$. Equation (5) is a first-order linear ODE for u_n and it can be solved by the standard integrating factor method:

$$u_n(t) = \exp\left[-\alpha_T\left(\frac{n\pi}{L}\right)^2 t\right] \int_0^t \exp\left[\alpha_T\left(\frac{n\pi}{L}\right)^2 s\right] \frac{\alpha_T}{K_T} q_n(s)\, ds. \tag{6}$$

Once the coefficients $u_n(t)$s are found, the solution $u(x,t)$ is given analytically by (4). However, the computation of (4) can be expensive if one uses direct summation. A more efficient numerical approach is to use the Fast Fourier Transform (FFT). In order to so, one first needs to even extend the problem from the domain $[0,L]$ to $[-L,L]$ and make it periodic with period $2L$. Then one can apply FFT and its inverse to find the numerical solution. Details of the implementation can be found in Tan's thesis (Tan, 2010).

An alternative way to solve the non-homogeneous 1-D heat equation (1) with insulating boundary conditions is to apply the Crank-Nicolson method. We begin by discretizing the interval $\left[0, L\right]$ into n subintervals with nodes

$$x_i = \left(i - \frac{1}{2}\right)\Delta x, \quad \Delta x = \frac{L}{n}, \quad i = 1, 2, \cdots, n \tag{7}$$

Then we approximate (1) with the Crank-Nicolson scheme:

$$\frac{u_i^{k+1} - u_i^k}{\Delta t} = \frac{\alpha_T}{2}\left[\frac{u_{i+1}{}^k - 2u_i^k + u_{i-1}{}^k}{\Delta x^2} + \frac{u_{i+1}{}^{k+1} - 2u_i^{k+1} + u_{i-1}{}^{k+1}}{\Delta x^2}\right] + \frac{\alpha_T}{2K_T}\left[q\left(x_i, t_k\right) + q\left(x_i, t_{k+1}\right)\right], \quad i = 1, 2, \cdots, n; \quad t_k = k\Delta t \tag{8}$$

and the insulating boundary conditions can be approximated by

$$u_0{}^k = u_1{}^k, \quad u_{n+1}{}^k = u_n{}^k, \quad \text{for all } k \geq 1. \tag{9}$$

In (8) $u_i^k \equiv u\left(i\Delta x, k\Delta t\right)$. The linear system (8) and (9) can be solved directly using MATLAB built-in function or the Thomas algorithm (Burden & Faires, 2005).

A third way to solve (1) is to use the commercial software COMSOL. COMSOL Multiphysics is a finite element analysis software for various physics and engineering applications.

In Figure 1(2) we plot the numerical solution of (1) obtained from these three different methods at $t = 1\,s$. As shown in Figure 1(2), the temperature rise along the rod from different methods agrees with each other very well. The two sharp peaks of the temperature rise occur near $x = 0.25$ and $x = 0.75$, which are the endpoints of the path of the dithering laser beam given in Equation (2). Since the beam moves with the prescribed path $x_c\left(t\right) = x_0 + a\sin 2\pi t/T$ where $x_0 = 0.5$, $a = 0.25$, $T = 1$, the velocity of the beam is $x_c'\left(t\right) = 0.5\pi\cos\left(2\pi t\right)$. Around the two endpoints $\sin\left(2\pi t\right) = \pm 1$ and

Table 1. Material properties of Steel AISI 4340 and parameters of the 1-D dithering laser beam

Property	Name	Value	Unit
Heat Capacity	C_p	475	J/(kg*K)
Density	ρ	7850	Kg/(m^3)
Thermal Conductivity	K_T	44.5	W/(m*K)
Thermal Diffusivity	α_T	$\frac{K_T}{\rho \cdot C_p}$	m^2/s
Melting Point		1783	K
Magnitude of Gaussian beam	I_0	1.0e9	W/(m^3)
Effective radius of Gaussian beam	r_0	0.02	m
Dithering frequency	$\frac{1}{T}$	1	Hz
Center of dithering	x_0	0.5	m
Dithering radius	a	0.25	m

$\cos\left(2\pi t\right)=0$. Consequently, the beam moves slower and stays longer near these two endpoints. Thus, the temperature is higher near the two endpoints. The material that we choose here is steel AISI 4340 with its physical properties listed in Table 1 and the parameters of the dithering laser beam are also given in Table 1.

Figure 1(3) depicts the maximum temperature rise as a function of the frequency of the dithering beam at a fixed time $t=0.1s$. Figure 1(3) shows that the maximum temperature rise acts as a decreasing function of the frequency of the dithering beam. In other words, the faster the dithering beam moves, the lower the maximum temperature rise. When the beam does not dither, the maximum temperature rise can be as high as $534K$. Once the beam dithers, the maximum temperature decreases quickly.

The asymptotic behavior of the maximum temperature rise can be predicted numerically by a least-squares curve fitting. In Figure 1(4) we show that the curve in Figure 1(3) can be well approximated by a function $T_{\max}=137.0864/\text{frequency}+51.6960$. Our result indicates that at a fixed time the maximum temperature rise decays asymptotically as a reciprocal function of the frequency of the dithering laser beam as the frequency goes to infinity. An intuitive physical explanation goes like this. After long time the temperature rise attains pseudo-steady state. If we observe the temperature rise at a fixed point, the temperature rise oscillates periodically as the beam passes through this point periodically. So the period of the temperature rise oscillation coincides with the period of the beam. The average temperature rise over one oscillation period is independent of the frequency of the beam. The maximum temperature rise over one oscillation period minus the average temperature rise is proportional to the period, which is inversely proportional to the frequency of the dithering laser beam.

Now we conduct an asymptotic analysis for an infinite long rod and show that the leading order term of the maximum temperature rise indeed is proportional to 1/frequency as the frequency of the dithering beam gets large. For simplicity, consider the following 1-D nonhomogeneous heat equation

$$\frac{\partial u}{\partial t}=\frac{\partial^2 u}{\partial x^2}+\frac{I_0}{r_0}\exp\left[-\frac{\left(x-a\sin\frac{2\pi t}{T}\right)}{4r_0^{\,2}}\right],\quad -\infty<x<\infty \tag{10}$$

with initial condition $u\left(x,0\right)=0\ \left(-\infty<x<\infty\right)$. The solution of (10) can be found by Duhamel's principle (Asmar, 2004; John, 1981):

$$u\left(x,t\right)=\int_0^t\int_{-\infty}^{\infty}\frac{1}{2\sqrt{\pi\left(t-s\right)}}\exp\left[-\frac{\left(x-y\right)^2}{4\left(t-s\right)}\right]\frac{I_0}{r_0}\exp\left[-\frac{\left(y-a\sin\frac{2\pi s}{T}\right)^2}{4r_0^{\,2}}\right]dyds. \tag{11}$$

We need to borrow a well-known result from probability theory (Hayter, 2002) to simplify (11).

Lemma. Suppose c_1 and c_2 are nonzero constants. Then

$$\int_{-\infty}^{\infty}\frac{1}{\sqrt{4\pi c_1^{\,2}}}\exp\left[-\frac{\left(x-y\right)^2}{4c_1^{\,2}}\right]\frac{1}{\sqrt{4\pi c_2^{\,2}}}\exp\left[-\frac{\left(y-z\right)^2}{4c_2^{\,2}}\right]dy=\frac{1}{\sqrt{4\pi\left(c_1^{\,2}+c_2^{\,2}\right)}}\exp\left[-\frac{\left(x-z\right)^2}{4\left(c_1^{\,2}+c_2^{\,2}\right)}\right] \tag{12}$$

In other words, the integral of the product of two Gaussian functions turns out to be another Gaussian function. The lemma expresses the fact that the convolution of two Gaussian (or normal) densities is another Gaussian. The proof of the lemma is straightforward and is skipped here. A simple 2-D version of the proof can be found in Zhou (2011).

Applying the lemma, we arrive at

$$\int_{-\infty}^{\infty} \exp\left[-\frac{\left(x-y\right)^2}{4\left(t-s\right)}\right]\exp\left[-\frac{\left(y-a\sin\frac{2\pi s}{T}\right)^2}{4r_0^{\,2}}\right]dy$$
$$=\frac{\sqrt{4\pi\left(t-s\right)}\sqrt{4\pi r_0^{\,2}}}{\sqrt{4\pi\left(t-s+r_0^{\,2}\right)}}\exp\left[-\frac{\left(x-a\sin\frac{2\pi s}{T}\right)^2}{4\left(t-s+r_0^{\,2}\right)}\right]. \quad (13)$$

Substituting (13) into (11) yields

$$u\left(x,t\right)=I_0\int_0^t\frac{1}{\sqrt{t-s+r_0^{\,2}}}\exp\left[-\frac{\left(x-a\sin\frac{2\pi s}{T}\right)^2}{4\left(t-s+r_0^{\,2}\right)}\right]ds. \quad (14)$$

Making a change of variables $s_{new}=t-s$ and then dropping the subscript, we obtain

$$u\left(x,t\right)=2I_0\int_0^t\frac{1}{\sqrt{h\left(s\right)}}\exp\left[-\frac{\left(x-a\sin z\right)^2}{h\left(s\right)}\right]ds \quad (15)$$

where

$$h\left(s\right)=4\left(s+r_0^{\,2}\right),\quad \varepsilon=T,\quad z=\frac{2\pi\left(t-s\right)}{\varepsilon}. \quad (16)$$

We wish to find the asymptotic expansion of $u\left(x,t\right)$ for small values of ε. To do so, consider the Fourier series expansion of

$$\exp\left[-\frac{\left(x-a\sin z\right)^2}{h\left(s\right)}\right]$$

as a function of z:

$$\exp\left[-\frac{\left(x-a\sin z\right)^2}{h\left(s\right)}\right]=\sum_{k=0}^{\infty}\left[a_k\cos\left(kz\right)+b_k\sin\left(kz\right)\right], \quad (17)$$

where a_k and b_k are the Fourier coefficients that depend on x,s and a.

Using (17), (15) becomes

$$u\left(x,t\right)=2I_0\left(U_0+\sum_{k=1}^{\infty}U_k\right), \quad (18)$$

where

$$U_0=\int_0^t\frac{1}{\sqrt{h\left(s\right)}}ds,$$
$$U_k=\int_0^t\frac{1}{\sqrt{h\left(s\right)}}\left[a_k\cos\left(k\frac{2\pi\left(t-s\right)}{\varepsilon}\right)+b_k\sin\left(k\frac{2\pi\left(t-s\right)}{\varepsilon}\right)\right]ds,\quad k>0. \quad (19)$$

Note that the leading term is U_0 which is $O\left(1\right)$ order, independent of ε. We continue to estimate U_k.

When $r_0\neq 0$, there is no singularity in the integrand function in U_k. Integration by parts yields

$$U_k=O\left(\varepsilon\right). \quad (20)$$

So asymptotically $u\left(x,t\right)$ behaves as $O\left(1\right)+O\left(\varepsilon\right)$ when $r_0\neq 0$, which is exactly what we have observed in Figure 4 even though the rod considered there is finite instead of infinite.

It is worthwhile to point out that if $r_0=0$, then there is a singularity in the integrand function in U_k. Applying the standard method of stationary phase (Bush, 1992) as in Zhou (2011), one can show that $u\left(x,t\right)$ then behaves as $O\left(1\right)+O\left(\sqrt{\varepsilon}\right)$ as $\varepsilon\to 0$, which shares the same scaling law as the 3-D semi-infinite case (Zhou, 2011).

Figure 4. (1) Snapshots of the normalized temperature rise for steel AISI 4340 induced by a rotating Gaussian beam where $\alpha_T = 1.19 \times 10^{-5}$. *(2) 2D maximum temperature rise versus frequency of the rotating laser beam for a thin steel AISI 4340 film. (3) The numerical results in (2) fitted by function* $T_{\max} = 293.5153/\text{frequency} + 50.8908$.

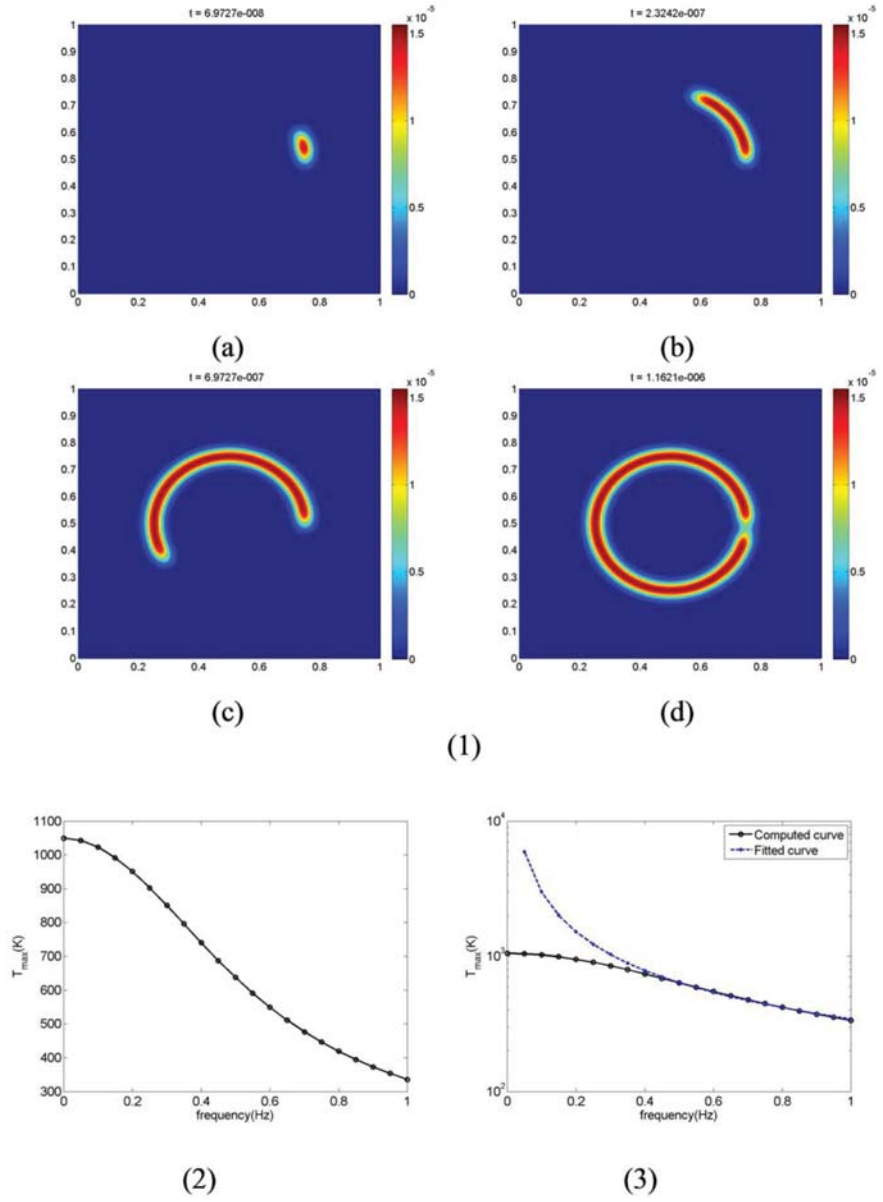

2-D MATHEMATICAL MODELING

When a laser beam shines on a two-dimensional rectangular-shaped thin film, the temperature rise of the film $u\left(x,y,t\right)$ is governed by

$$\frac{\partial u}{\partial t}=\alpha_T\left[\frac{\partial^2 u}{\partial x^2}+\frac{\partial^2 u}{\partial y^2}\right]+\frac{\alpha_T}{K_T}f\left(x,y,t\right),\quad 0\le x\le L_x, 0\le y\le L_y, \tag{21}$$

where the heat source $f\left(x,y,t\right)$ due to a rotating laser beam can be written as

$$f\left(x,y,t\right)=\frac{I_0}{2\pi d^2}\exp\left[-\frac{\left(x-x_c\left(t\right)\right)^2+\left(y-y_c\left(t\right)\right)^2}{2d^2}\right],$$
$$x_c\left(t\right)=x_0+a\cos\frac{2\pi t}{T},\quad x_0=\frac{L_x}{2},$$
$$y_c\left(t\right)=y_0+b\sin\frac{2\pi t}{T},\quad y_0=\frac{L_y}{2}. \tag{22}$$

In the case that $b=0$ in (22) the laser beam is called a dithering beam. The 2-D rotating laser beam and the finite thin film are illustrated in Figure 2(1) while the heat source $f\left(x,y,t\right)$ given in (22) is shown in Figure 2(2).

The boundary conditions impose the insulating condition:

$$\frac{\partial u}{\partial x}=0 \text{ at } x=0 \text{ or } L_x,$$
$$\frac{\partial u}{\partial y}=0 \text{ at y}=0 \text{ or } L_y, \tag{23}$$

and the initial condition is

$$u\left(x,y,0\right)=0. \tag{24}$$

Like 1-D case, one can derive the analytical solution to the initial-boundary-value problem (IBVP) (21)-(24) using the eigenfunction expansion method and end up with double summation, which is computationally expensive. An alternative approach is to use Fast Fourier Transform (FFT). Again, one first needs to even extend the problem from the rectangular domain $\left[0,L_x\right]\times\left[0,L_y\right]$ to a larger domain $\left[-L_x,L_x\right]\times\left[-L_y,L_y\right]$ and then apply FFT and its inverse to obtain the numerical solution.

Another straightforward method to solve (21)-(24) is to apply the Crank-Nicolson scheme:

$$\begin{aligned}\frac{u_{i,j}^{\,k+1}-u_{i,j}^{\,k}}{\Delta t}&=\frac{\alpha_T}{2}\left[\frac{u_{i+1,j}^{\,k}-2u_{i,j}^{\,k}+u_{i-1,j}^{\,k}}{\Delta x^2}+\frac{u_{i+1,j}^{\,k+1}-2u_{i,j}^{\,k+1}+u_{i-1,j}^{\,k+1}}{\Delta x^2}\right]\\&+\frac{\alpha_T}{2}\left[\frac{u_{i,j+1}^{\,k}-2u_{i,j}^{\,k}+u_{i,j-1}^{\,k}}{\Delta y^2}+\frac{u_{i,j+1}^{\,k+1}-2u_{i,j}^{\,k+1}+u_{i,j-1}^{\,k+1}}{\Delta y^2}\right]\\&+\frac{\alpha_T}{2K_T}\left[f\left(x_i,y_j,t_k\right)+f\left(x_i,y_j,t_{k+1}\right)\right],\end{aligned} \tag{25}$$

where the grid points are given by

$$x_i=\left(i-\frac{1}{2}\right)\Delta x,\quad \Delta x=\frac{L_x}{n},\quad i=1,2,\cdots,n$$
$$y_j=\left(j-\frac{1}{2}\right)\Delta y,\quad \Delta y=\frac{L_y}{m},\quad j=1,2,\cdots,m$$
$$t_k=k\Delta t,\quad k=0,1,2,\cdots \tag{26}$$

and $u_{i,j}^{\,k}\equiv u\left(x_i,y_j,t_k\right)$. The boundary conditions are approximated by

$$u_{0,j}^{\,k}=u_{1,j}^{\,k},\quad u_{n+1,j}^{\,k}=u_{n,j}^{\,k},$$
$$u_{i,0}^{\,k}=u_{i,1}^{\,k},\quad u_{i,m+1}^{\,k}=u_{i,m}^{\,k}. \tag{27}$$

The linear system (25) together with (27) can be solved efficiently in MATLAB by taking advantage of the built-in sparse matrix operations.

A third method to solve the 2D problem (21)-(24) is to apply COMSOL directly.

Before we present our numerical results, we would like to investigate the effects of physical parameters on the solution of (21). In

Figure 2. (1) A schematic 2-D diagram shows a rotating laser beam and the finite work place. (2) The plot of the heat source due to a Gaussian beam.

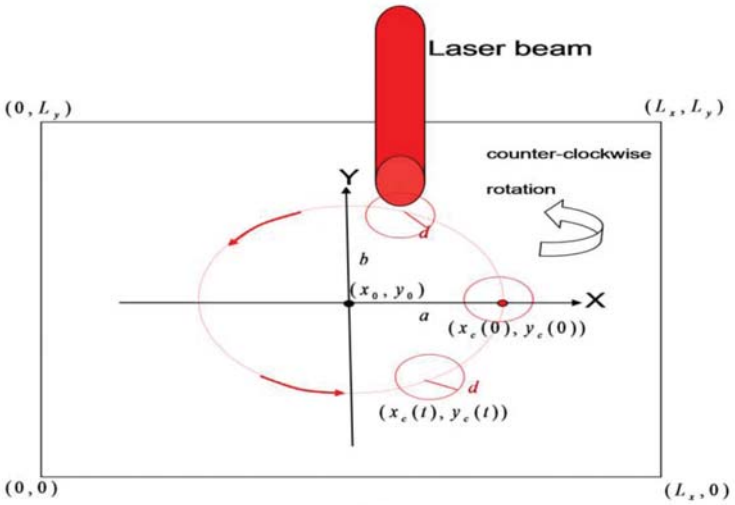

(1)

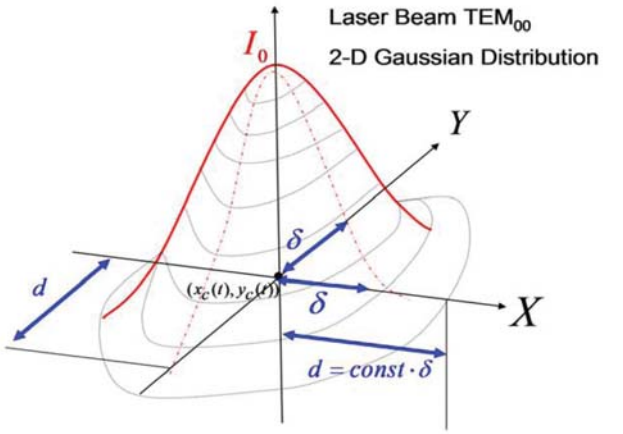

$$\text{Heat source: } f(x,y,t) = \frac{I_0}{2\pi d^2} e^{\frac{-((x-x_c(t))^2+(y-y_c(t))^2)}{2d^2}}$$

(2)

order to do so, we first rescale the time variable as $t_{new} = \alpha_T t$ and then drop the subscript. Then (21) can be rewritten as

$$\frac{\partial u}{\partial t} = \left[\frac{\partial^2 u}{\partial x^2} + \frac{\partial^2 u}{\partial y^2}\right] + \frac{1}{K_T} f\left(x, y, \frac{t}{\alpha_T}\right). \tag{28}$$

Substituting (22) into (28), we obtain

$$\frac{\partial u}{\partial t} = \left[\frac{\partial^2 u}{\partial x^2} + \frac{\partial^2 u}{\partial y^2}\right] + \frac{I_0}{2\pi d^2 K_T} \exp\left[-\frac{\left(x - \frac{L_x}{2} - a\cos\frac{2\pi t}{\alpha_T T}\right)^2 + \left(y - \frac{L_y}{2} - b\sin\frac{2\pi t}{\alpha_T T}\right)^2}{2d^2}\right]. \tag{29}$$

Let $\tilde{u}$ denote the solution to the following IBVP problem

$$\frac{\partial \tilde{u}}{\partial t} = \left[\frac{\partial^2 \tilde{u}}{\partial x^2} + \frac{\partial^2 \tilde{u}}{\partial y^2}\right] + \exp\left[-\frac{\left(x - \frac{L_x}{2} - a\cos\frac{2\pi t}{\alpha_T T}\right)^2 + \left(y - \frac{L_y}{2} - b\sin\frac{2\pi t}{\alpha_T T}\right)^2}{2d^2}\right], \tag{30}$$

$$\tilde{u}(x, y, 0) = 0,$$
$$\frac{\partial \tilde{u}}{\partial x} = 0 \text{ at } x = 0 \text{ or } L_x,$$
$$\frac{\partial \tilde{u}}{\partial y} = 0 \text{ at y} = 0 \text{ or } L_y.$$

Then it is obvious that the solution to (28) with same initial/boundary conditions is related to the solution of (30) through the relationship:

$$u(x, y, t) = \frac{I_0}{2\pi d^2 K_T} \tilde{u}(x, y, t). \tag{31}$$

So from a computational point of view, one should solve (30) to obtain the normalized solution $\tilde{u}(x, y, t)$ and then multiply the normalized solution by a constant factor $I_0 / 2\pi d^2 K_T$ to get the solution for (28), or equivalently (21). From this simple analysis, it is clear that the effect of the thermal diffusivity α_T is to change the effective frequency of rotation and the effect of the intensity of the laser beam I_0 and the thermal conductivity K_T is to rescale the temperature distribution by a factor proportional to I_0 / K_T. The same argument applies to the 1D and 3D cases.

Now we show some numerical results. In Figure 3 we take the snapshots of the numerical solutions of the problem (30) with $\alpha_T = 0.1$ at various times where the parameters for the rotating laser beam are listed in Table 2. Our numerical experiments have shown that the solutions obtained from the Crank-Nicolson method, FFT and COMSOL all agree with each other (Tan, 2010), which we do not present individually here. We only give the FFT results in Figure 3. One can see from Figure 3 that the maximum temperature rise increases as time increases. The hottest spot is the place that is directly hit by the laser beam.

Figure 4(1) shows the numerical results of (30) for steel AISI 4340 where $\alpha_T = 1.19 \times 10^{-5}$ (refer to Table 1). Due to the small value of α_T heat does not diffuse fast enough and consequently a hot ring starts to form. Using the values listed in Table 2, we find that the normalized maximum temperature in Figure 4(1)d corresponds to a value $270.6794K$ after multiplying by the factor $I_0 / 2\pi d^2 K_T$. Similarly, the corresponding time of Figure 4(1)d is $0.0977s$ after multiplying by $1/\alpha_T$.

In Figure 4(2) we plot the maximum temperature rise for different values of the frequency (i.e. the reciprocal of the period T) at a fixed time $t = 0.1s$ for a thin steel film with the shape of a unit square. As the frequency increases, the maximum temperature rise decreases and the asymptotic behavior of this decrease is depicted in Figure 4(3) by a fitting function $T_{\max} = 293.5153/\text{frequency} + 50.8908$. Figure 4(3) implies that the maximum temperature rise is proportional to the reciprocal of the frequency as the frequency gets large.

Figure 3. Snapshots of the temperature rise induced by a rotating Gaussian beam at various times where $\alpha_T = 0.1$

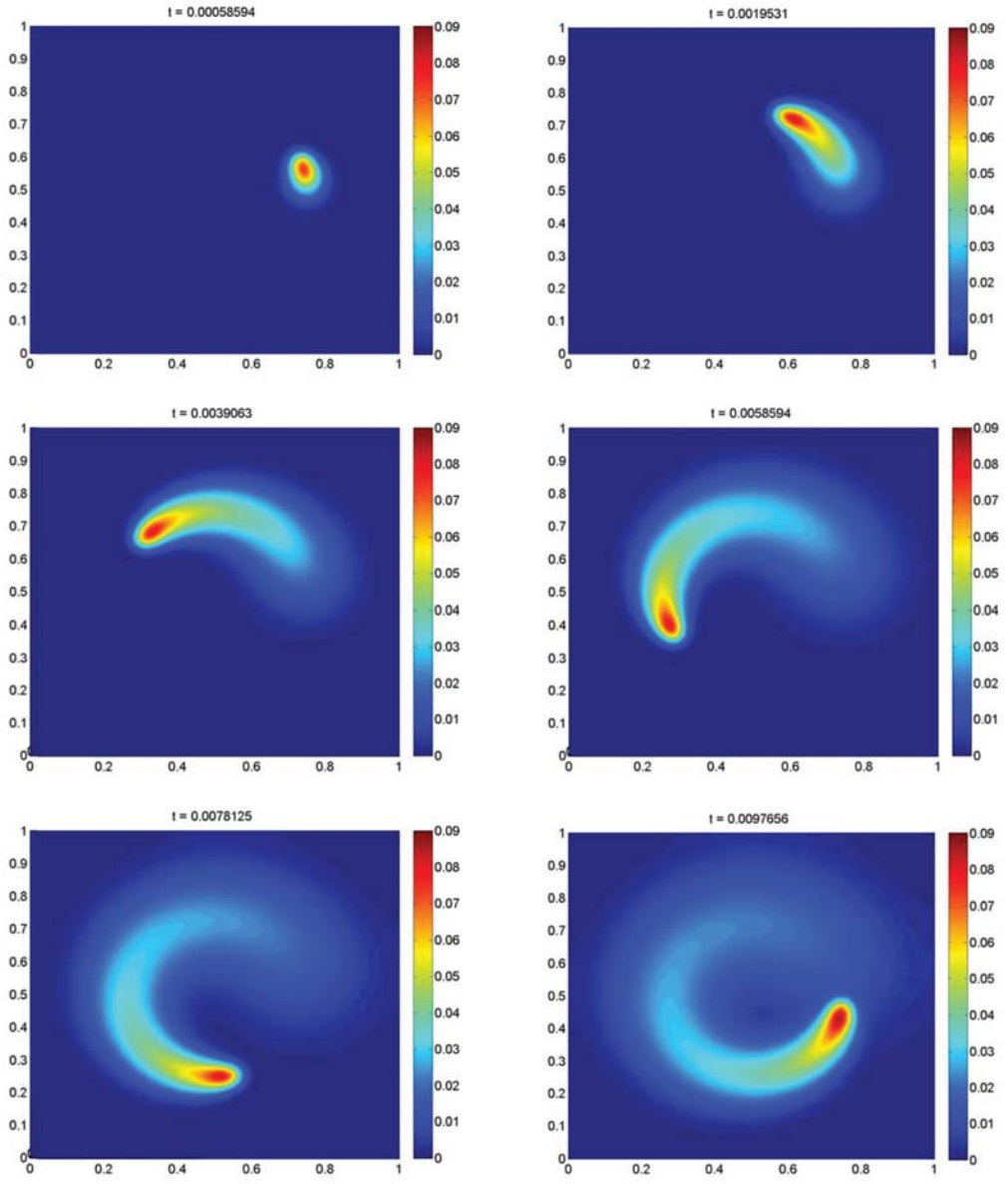

In Figure 5(1) we give the snapshots of the temperature rise when the laser beam is dithering (where $a = 0.25$ and $b = 0$ in equation (22)). Here $\alpha_T = 0.1$ and the solutions are obtained by solving (30) with FFT. Note that the dithering beam moves at its slowest speed at the endpoints of its trajectory so these two endpoints are exposed directly to the beam longer than other places.

In Figure 5(2) we compare the maximum temperature rise against the frequency of the rotating and dithering beams for a square-shaped

Table 2. Parameters of the 2-D rotating laser beam

Parameter	Value	Unit
α_T	1	m^2/s
K_T	1	W/(m*k)
I_0	1.0e8	W/m^3
d	0.02	m
L_x	1	m
L_y	1	m
x_0	0.5	m
a	0.25	m
b	0.25	m
period	1	s

thin steel film at $t = 0.1s$. As the frequency increases, the maximum temperature rise decreases. The maximum temperature rise corresponding to the rotating beam drops much faster than the one induced by the dithering beam for the same frequency. It implies that rotating a beam is more effective than dithering a beam if one desires a lower temperature rise.

3-D MATHEMATICAL MODELING

In the case of a rectangular prism hitting by a laser beam, the temperature rise on the solid body is described by

$$\frac{\partial u}{\partial t} = \alpha_T \left[\frac{\partial^2 u}{\partial x^2} + \frac{\partial^2 u}{\partial y^2} + \frac{\partial^2 u}{\partial z^2}\right] + \frac{\alpha_T}{K_T} q\left(x, y, z, t\right), \quad 0 \le x \le L_x, 0 \le y \le L_y, 0 \le z \le L_z \tag{32}$$

where the heat source $q\left(x, y, z, t\right)$ due to the rotating laser beam can be modeled as

$$q\left(x, y, z, t\right) = f\left(x, y, t\right)\delta\left(z\right). \tag{33}$$

Here $f\left(x, y, t\right)$ is given in equation (22) and the delta function in z expresses the assumption that all the energy is absorbed at the surface $z = 0$ which is hit directly by the beam. The boundary conditions are insulating and the initial condition is zero.

Our numerical experiments in 1D and 2D cases have indicated that COMSOL yields reliable results. So for 3D case, instead of using FFT or the Crank-Nicolson method, we use COMSOL alone to compute the temperature rise induced by a rotating laser beam. The parameters of the 3D rotating laser beam are specified in Table 3. Details on how to implement COMSOL can be found in Tan (2010).

Figure 6(1) gives several snapshots of the temperature rise induced by a rotating Gaussian laser beam at different times within one time period. The hottest spot is the place that is hit directly by the laser beam, as in the 2D case. The maximum temperature rise reaches $1468K$ at time $t = 1s$. Those points far away from the heat source have little temperature rise. Figure 6(2) is similar to Figure 6(1), but for a different period $0.1s$. Figure 6(2) shows a maximum temperature rise drops from $1468K$ with period $1s$ to $670K$ with period $0.1s$, which is about 54% reduction in the maximum temperature rise. Therefore, the maximum temperature rise can be significantly reduced by increasing the frequency of the rotating laser beam.

In Figure 7(1) we show the temperature rise at different layers at time $t = 1s$ corre-

Figure 5. (1) Snapshots of the temperature rise induced by a dithering Gaussian beam at various times with $\alpha_T = 0.1$. *(2) Comparison of the 2D maximum temperature rise versus frequency of the rotating and dithering laser beams for a square-shaped thin steel film.*

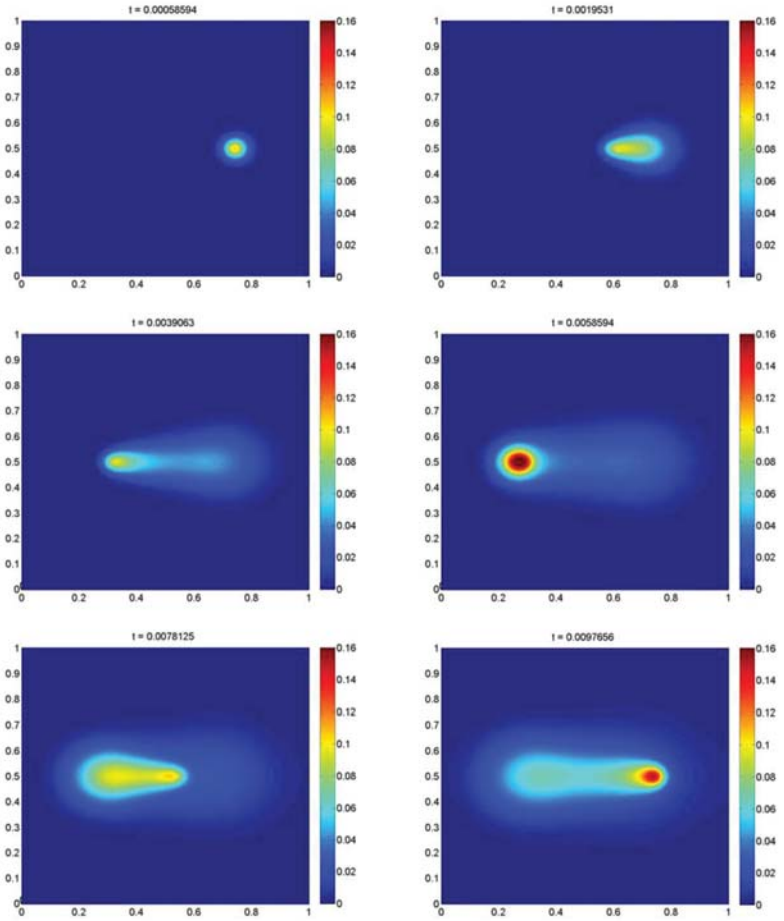

(1)

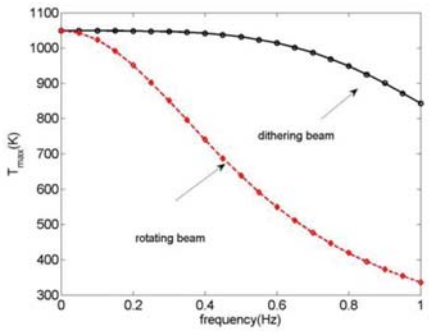

(2)

Table 3. Parameters of the 3-D rotating laser beam

Input	Value	Unit
I_0	5.0e5	W/m^2
d	0.02	m
L_x	1	m
L_y	1	m
x_0	0.5	m
y_0	0.5	m
a	0.25	m
b	0.25	m
period	1	s

sponding to the results in Figure 6(1). It is observed that heat does not spread out downward quickly and there is almost no temperature rise for the body part that is more than $0.1m$ below the top surface. This is because the diffusivity of steel AISI 4340 is quite small (recall $\alpha_T = 1.19 \times 10^{-5}$) and thus heat diffuses very slowly. For materials with larger diffusivity we observe that the heat spreads out fast and the temperature rise occurs in other layers below the top surface.

Finally, the relationship between the maximum temperature rise and the frequency of the rotating laser beam is depicted in Figure 7(2). As expected, the increase of the frequency of the rotating laser beam leads to a decrease of the maximum temperature rise. In Figure 7(3) we fit the numerical results in Figure 7(2) by a function

$$T_{\max} = \frac{1228.3}{\text{frequency}} + 522.5 \tag{34}$$

using the lease-squares approach. The good agreement between the fitted curve and the numerical results indicates that the maximum temperature rise is inversely proportional to the frequency of the rotating beam.

CONCLUSION AND FUTURE EFFORTS

We have calculated the temperature rise induced by a rotating or dithering Gaussian laser beam for a finite body in different spatial dimensions. We have confirmed that for a finite solid the maximum temperature rise can be reduced by increasing the frequency of a rotating or dithering beam. Furthermore, the temperature rise induced by a rotating laser beam is smaller than the one induced by a dithering laser beam. We have given the asymptotic behavior of the maximum temperature rise as a function of the frequency of the dithering or rotating laser beam. Future efforts will include (1) experimentally determining the actual temperature profile induced by a rotating or dithering laser beam on different materials and comparing the measured temperature profiles to the predicted profiles; (2) using stochastic differential equations to revisit the problem; (3) investigating the temperature rise in a two-layer structure.

ACKNOWLEDGMENT

H. Zhou would like to thank Mr. Peter Morrison and the Office of Naval Research (ONR) for supporting this work. We thank the anonymous referees for their helpful suggestions and comments.

Figure 6. Snapshots of the temperature rise on a steel AISI 4340 box induced by a rotating Gaussian laser beam using COMSOL (1) with period 1s; (2) with period 0.1s

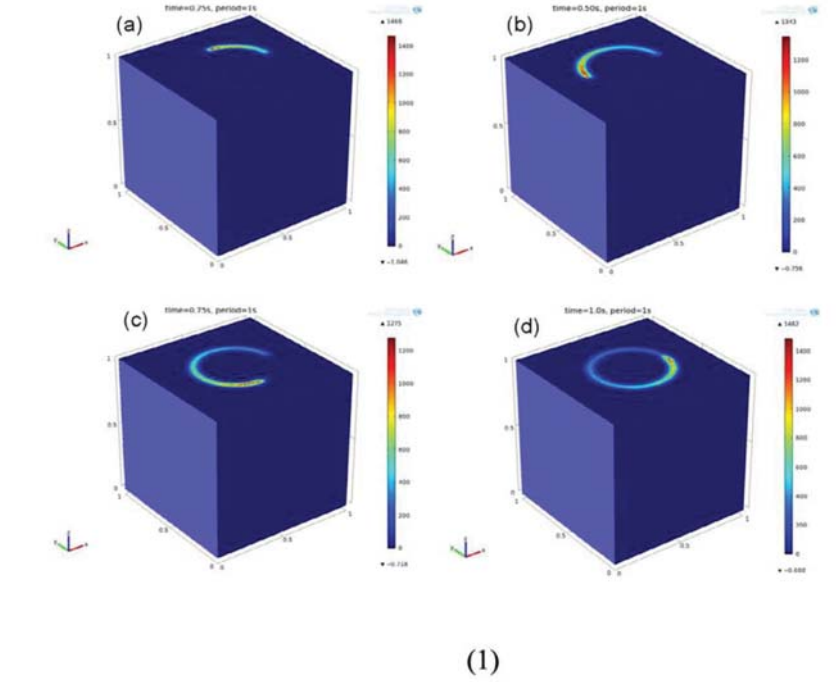

(1)

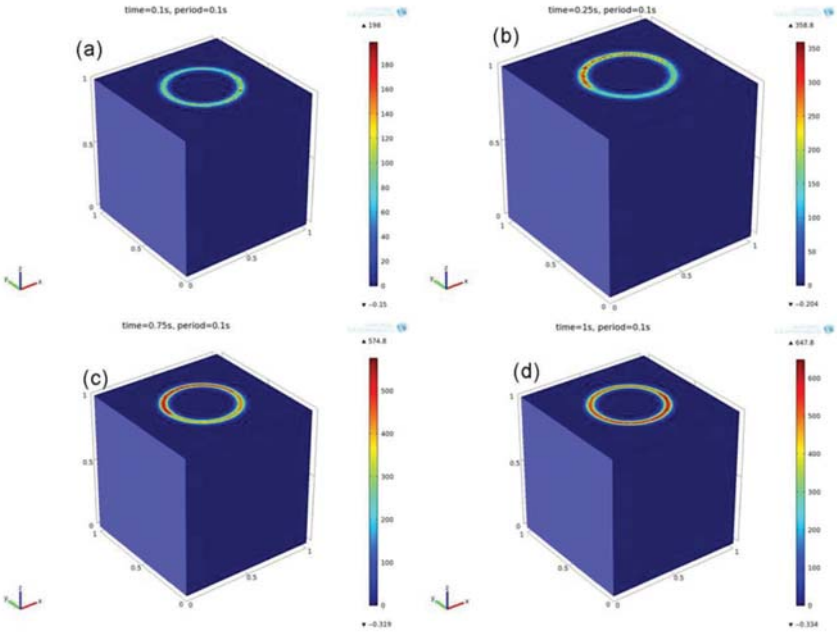

(2)

Figure 7. (1) Temperature rise of a box made of steel AISI 4340 at different depth corresponding to Figure 6 (1): (a) $z = 1$ *(top surface hit directly by the laser beam) (b)* $z = 0.99$ *(c)* $z = 0.95$ *and (d)* $z = 0.90$ *. (2) 3D maximum temperature rise of steel AISI 4340 versus frequency of the rotating laser beam. (3) The numerical results in (2) are fitted by the function* $T_{\max} = 1228.3/\text{frequency} + 522.5$ *.*

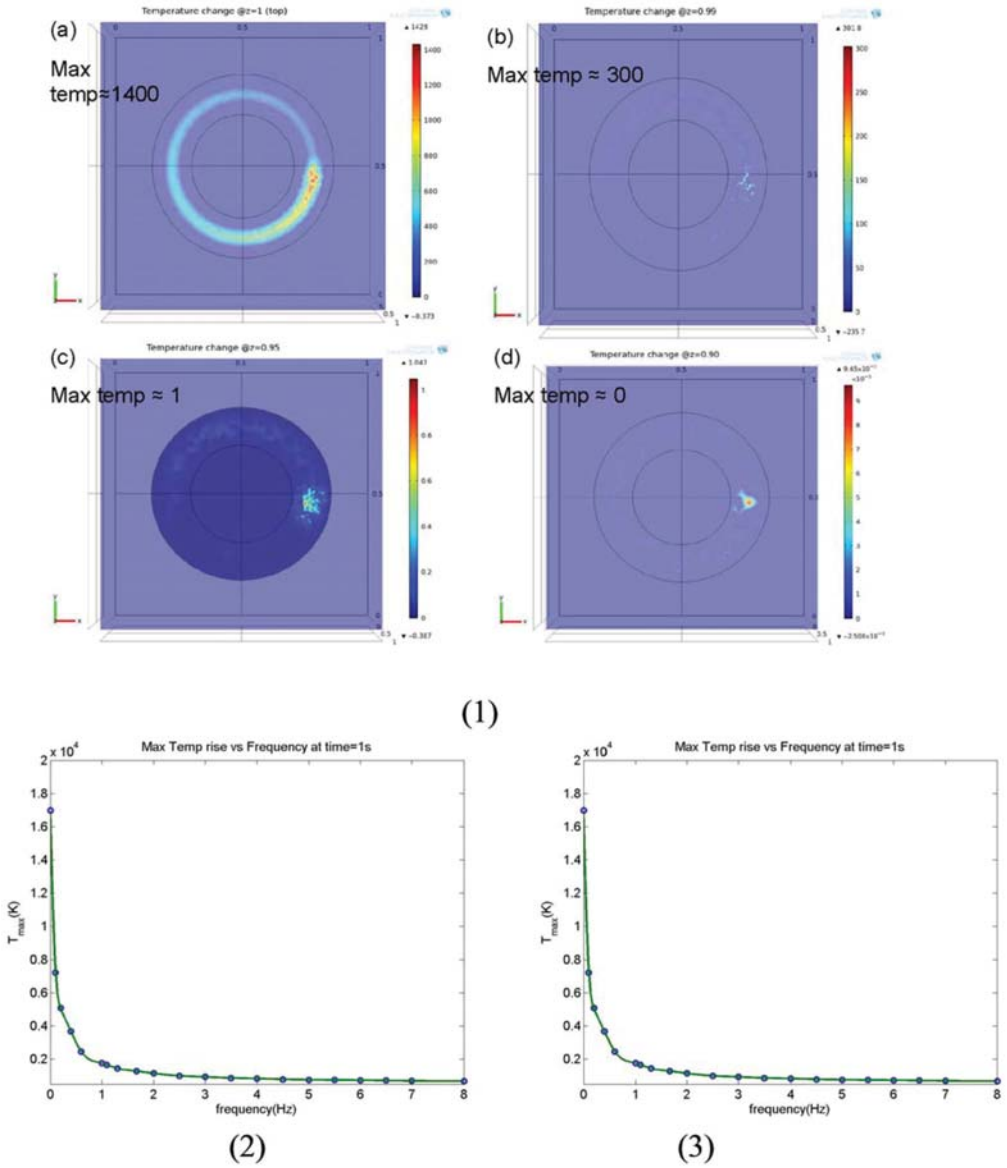

REFERENCES

Araya, G., & Gutierrez, G. (2006). Analytical solution for a transient, three-dimensional temperature distribution due to a moving laser beam. *International Journal of Heat and Mass Transfer*, *49*, 4124–4131. doi:10.1016/j.ijheatmasstransfer.2006.03.026

Asmar, N. H. (2004). *Partial differential equations with fourier series and boundary value problems* (2nd ed.). Upper Saddle River, NJ: Prentice Hall.

Bertolotti, M., & Sibilia, C. (1981). Depth and velocity of the laser-melted front from an analytical solution of the heat conduction equation. *IEEE Journal of Quantum Electronics*, *17*, 1980–1989. doi:10.1109/JQE.1981.1070643

Burden, R. L., & Faires, J. D. (2005). *Numerical Analysis* (8th ed.). Boston, MA: Brooks/Cole.

Burgener, M. L., & Reedy, R. E. (1982). Temperature distributions produced in a two-layer structure by a scanning cw laser or electron beam. *Journal of Applied Physics*, *53*, 4357–4363. doi:10.1063/1.331216

Bush, A. W. (1992). *Perturbation methods for engineers and scientists*. CRC Press.

Calder, I. D., & Sue, R. (1982). Modeling of cw laser annealing of multilayer structures. *Journal of Applied Physics*, *53*, 7545–7550. doi:10.1063/1.330123

Cline, H. E., & Anthony, T. R. (1977). Heat treating and melting material with a scanning laser or electron beam. *Journal of Applied Physics*, *48*, 3895–3900. doi:10.1063/1.324261

Hayter, A. J. (2002). *Probability and statistics for engineers and scientists*. Pacific Grove, CA: Duxbury.

John, F. (1981). *Partial differential equations*. Springer.

Lax, M. (1977). Temperature rise induced by a laser beam. *Journal of Applied Physics*, *48*, 3919–3924. doi:10.1063/1.324265

Lax, M. (1978). Temperature rise induced by a laser beam II: The nonlinear case. *Applied Physics Letters*, *33*, 786–788. doi:10.1063/1.90505

Moody, J. E., & Hendel, R. H. (1982). Temperature profiles induced by a scanning cw laser beam. *Journal of Applied Physics*, *53*, 4364–4371. doi:10.1063/1.331217

Sanders, D. J. (1984). Temperature distributions produced by scanning Gaussian laser beams. *Applied Optics*, *23*, 30–35. doi:10.1364/AO.23.000030 PMID:18204509

Sistaninia, M., Sistaninia, M., & Moeanodini, H. (2009). Laser forming of plates using rotating and dithering beams. *Computational Materials Science*, *45*, 480–488. doi:10.1016/j.commatsci.2008.11.011

Tan, T. (2010). *Temperature rise induced by a rotating/dithering laser beam on a finite solid*. Naval Postgraduate School, Master Thesis.

Zhou, H. (2011). Temperature rise induced by a rotating or dithering laser beam. *Advanced Studies in Theoretical Physics*, *5*(10), 443–468.

Tsuwei Tan got his B.S. from U.S. Naval Academy in 2004 and Master degree from Naval Postgraduate School in December 2010 under the supervision of Dr. Zhou. Mr. Tan is currently a Lieutenant in the Republic of China Navy (Taiwanese Navy).

Hong Zhou is an associate professor in the Department of Applied Mathematics at Naval Postgraduate School. Dr. Zhou received her Ph.D. in Applied Mathematics from University of California, Berkeley in 1996 and spent three years as a postdoctoral fellow at University of North Carolina, Chapel Hill. She taught at University of California, Santa Cruz for five years before she joined Naval Postgraduate School. Her current research interests include complex fluids and C-DEW related mathematical problems. She has published more than forty papers in journals such as *Physics of Fluids, Nonlinearity, Journal of Non-Newtonian Fluid Mechanics, Liquid Crystals*, and *SIAM Journal of Applied Mathematics*.